

OPTICAL AND SUPERSOFT X-RAY LIGHT CURVE MODELS OF CLASSICAL NOVA V2491 CYGNI: A NEW CLUE TO THE SECONDARY MAXIMUM

IZUMI HACHISU

Department of Earth Science and Astronomy, College of Arts and Sciences, University of Tokyo, Komaba, Meguro-ku, Tokyo 153-8902, Japan

AND

MARIKO KATO

Department of Astronomy, Keio University, Hiyoshi, Kouhoku-ku, Yokohama 223-8521, Japan

to appear in the *Astrophysical Journal, Letters*

ABSTRACT

V2491 Cygni (Nova Cygni 2008 No.2) was detected as a transient supersoft X-ray source with the *Swift* XRT as early as 40 days after the outburst, suggesting a very massive white dwarf (WD) close to the Chandrasekhar limit. We present a unified model of near infrared, optical, and X-ray light curves for V2491 Cyg, and have estimated, from our best-fit model, the WD mass to be $1.3 \pm 0.02 M_{\odot}$ with an assumed chemical composition of the envelope, $X = 0.20$, $Y = 0.48$, $X_{\text{CNO}} = 0.20$, $X_{\text{Ne}} = 0.10$, and $Z = 0.02$ by mass weight. We strongly recommend detailed composition analysis of the ejecta because some enrichment of the WD matter suggests that the WD mass does not increase like in RS Oph, which is a candidate of Type Ia supernova progenitors. V2491 Cyg shows a peculiar secondary maximum in the optical light curve as well as V1493 Aql and V2362 Cyg. Introducing magnetic activity as an adding energy source to nuclear burning, we propose a physical mechanism of the secondary maxima.

Subject headings: novae, cataclysmic variables — stars: individual (V1493 Aql, V2362 Cyg, V2491 Cyg) — stars: mass loss — X-rays: binaries

1. INTRODUCTION

Classical novae show a wide variety of timescales and shapes in the optical light curves (e.g., Payne-Gaposchkin 1957). Among various shapes of nova light curves, V1493 Aql (Nova Aquilae 1999 No.1) shows an impressive secondary maximum about 50 days after the outburst (e.g., Bonifacio et al. 2000; Venturini et al. 2004), although the physical mechanism of the secondary maximum is not understood yet. Recent two novae, V2362 Cyg (Nova Cygni 2006) and V2491 Cyg (Nova Cygni 2008 No.2), also show a similar type of single secondary maximum, at about 250 and 15 days after the outburst, respectively. These three novae form a wide variety set of timescales, i.e., about 15, 50, and 250 days at the secondary maximum and of secondary peak heights, i.e., 1.1, 2.8, and 3.6 mag, respectively, (see, e.g., Kimeswenger et al. 2008), which provide us a new clue to the mechanism of the secondary maxima.

In this Letter, we propose a strong magnetic activity as the mechanism of the secondary maxima observed in V2491 Cyg, V1493 Aql, and V2362 Cyg, using the white dwarf (WD) parameters obtained from light curve fittings based on an optically thick wind model of nova outbursts (Kato & Hachisu 1994). In §2, we briefly describe our numerical method and light curve fitting of V2491 Cyg. In §3, we propose an idea of strong magnetic activity in the WD envelope and estimate the timescales of the secondary maxima. V1493 Aql and V2362 Cyg show very different timescales of the secondary maximum, both of which are also explained by the same mechanism in §4. Conclusions follow in §5.

2. MODELING OF NOVA OUTBURSTS

2.1. Optically thick wind model

After a thermonuclear runaway sets in on a mass-accreting WD, its photospheric radius expands greatly to $R_{\text{ph}} \gtrsim 100 R_{\odot}$ and the WD envelope settles in a steady-state. We have followed evolutions of novae by connecting steady state solutions along the decreasing envelope mass sequence. We solve a set of equations, that is, the continuity, equation of motion, radiative diffusion, and conservation of energy, from the bottom of the hydrogen-rich envelope through the photosphere assuming spherical symmetry. Winds are accelerated deep inside the photosphere so that they are called “optically thick winds.” As one of the boundary conditions for our numeral code, we assume that photons are emitted at the photosphere as a blackbody with the photospheric temperature of T_{ph} . X-ray flux is estimated directly from the blackbody emission, but infrared and optical fluxes are calculated from free-free emission by using the physical values of our wind solutions. We neglect the effect of ash helium layer, which may be piled up beneath the hydrogen burning zone, for all nova calculations except the RS Oph case (Hachisu et al. 2007). Our method and various physical properties of these wind solutions have already been published (e.g., Hachisu & Kato 2001a,b, 2004, 2006, 2007; Hachisu et al. 1996, 1999a,b, 2000, 2003, 2007, 2008; Kato 1983, 1997, 1999; Kato & Hachisu 1994).

The light curves of our optically thick wind model are parameterized by the WD mass (M_{WD}), chemical composition of the envelope (X , Y , X_{CNO} , X_{Ne} , and Z), and the envelope mass ($\Delta M_{\text{env},0}$) at the outburst (day 0). Details of our light curve fittings are described in Hachisu & Kato (2006, 2007) and Hachisu et al. (2007, 2008).

2.2. Light curve fitting (V2491 Cyg)

V2491 Cyg was discovered by Nishiyama and Kabashima at mag 7.7 on 2008 April 10.728 UT (Nakano et al. 2008). The nova was not detected on 2008 April 8.831 UT (limiting mag 14). The exact outburst day is unknown, so we assume here that $t_{\text{OB}} = 2454566.0$ (April 9.5 UT) is the outburst day (day

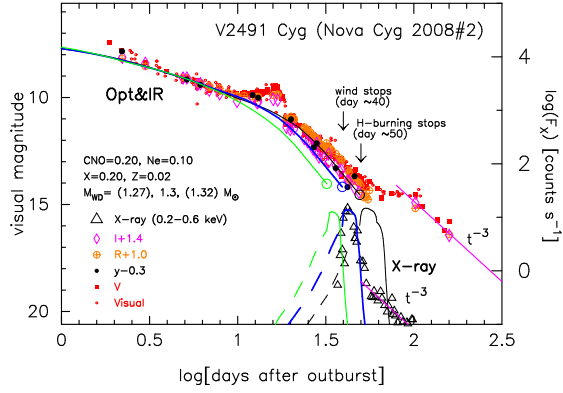


FIG. 1.— Model light curves of V2491 Cyg for three white dwarf masses, $1.32 M_{\odot}$ (green line), $1.3 M_{\odot}$ (thick blue line), and $1.27 M_{\odot}$ (thin black line), together with the observations. See Hachisu & Kato (2006) for more details of light curve fitting. Two arrows indicate epochs when the wind stops (day 40) and when the hydrogen shell-burning ends (day 50) in the $1.3 M_{\odot}$ WD model. *Dashed lines*: Supersoft X-rays are probably not detected during the wind phase because of self-absorption by wind itself (see, e.g. Hachisu & Kato 2003b). Large open circles at the right end of each optical light curve denote the epoch when the optically thick wind stops. We obtain the best-fit model for the envelope chemical composition of $X = 0.20$, $Y = 0.48$, $X_{\text{CNO}} = 0.20$, $X_{\text{Ne}} = 0.10$, and $Z = 0.02$. *Large open triangles*: Observational X-ray (0.2–0.6 keV) count rates obtained with *Swift* (Page et al. 2009). Optical and near IR observational data of *I* (open diamonds), *R* (circles with a plus), *V* (filled squares), *y* (filled circles), and visual (small open circles) are taken from AAVSO (American Association of Variable Star Observers) and VSOLJ (Variable Star Observers League in Japan). The $F_{\lambda} \propto t^{-3}$ law (magenta) is added for the nebular phase, i.e., after the wind stops, where t is the time after the outburst.

0). The orbital period of $P_{\text{orb}} = 0.0958$ days was derived by Baklanov et al. (2008) from the modulations with an amplitude of 0.03–0.05 mag.

The rise or decay time of supersoft X-ray flux is an important indicator of the WD mass (e.g., Hachisu & Kato 2006, 2007; Hachisu et al. 2008). The best fit model with the *Swift* observation (Page et al. 2009) is the WD mass of $1.3 \pm 0.02 M_{\odot}$ as shown in Figure 1. Here we adopt the chemical composition of $X = 0.20$, $Y = 0.48$, $X_{\text{CNO}} = 0.20$, $X_{\text{Ne}} = 0.10$, and $Z = 0.02$ to reproduce a short (10 days) supersoft X-ray duration (see Hachisu & Kato 2006, 2007; Hachisu et al. 2007, 2008, for dependence on chemical composition).

Figure 1 also shows optical and near IR light curves of the *I*, *R*, *V*, *y*, and visual magnitudes. Our theoretical light curves of free-free emission reasonably fit with the observation until day ~ 50 except the secondary peak. After that, the observational data deviate probably due to the contribution of nebular emission lines.

Thus we conclude that the WD of V2491 Cyg is as massive as $1.3 M_{\odot}$ from our light curve fittings with the supersoft X-ray, optical, and near IR data. This WD mass of V2491 Cyg is a bit less massive but comparable to that of the recurrent nova RS Oph (Hachisu et al. 2007), the supersoft X-ray duration of which lasted 60 days starting from day 30, much longer than the 10 days in V2491 Cyg. Hachisu et al. (2007) explained this long duration of supersoft X-ray phase of RS Oph by incorporating heat flux from a hot helium layer underneath the hydrogen burning zone, which develops in mass-increasing WDs. In V2491 Cyg, however, the supersoft X-ray phase lasts only 10 days, indicating that no thick helium layer develops beneath the hydrogen burning zone and, therefore, the WD mass is not increasing (see discussion in Hachisu et al. 2007). Tomov et al. (2008) suggested a possibility that V2491 Cyg is a recurrent nova, for which we ex-

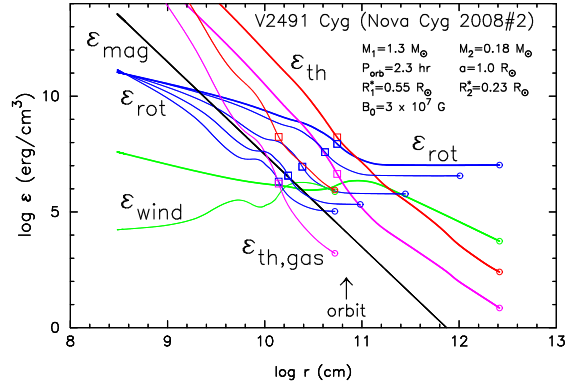


FIG. 2.— Five energy densities of the WD envelope are plotted against the radius, i.e., thermal energy (ϵ_{th} : red), thermal gas energy ($\epsilon_{\text{th,gas}}$: magenta), rotational kinetic energy (ϵ_{rot} : blue), magnetic energy (ϵ_{mag} : black), and wind kinetic energy (ϵ_{wind} : green). Five sequential stages are plotted for ϵ_{rot} but only two stages [the first (thick solid) and the last (thin solid)] for the other energy densities. Open circles indicate the photosphere while open squares correspond to the critical point of each wind solution. Various parameters are summarized in the figure.

pect that the WD mass is increasing (Hachisu & Kato 2001b). One of the strongest clues to this question is the chemical composition of the ejecta. We strongly recommend composition analysis of V2491 Cyg to clarify whether or not the ejecta are contaminated by WD matter. *Suzaku* X-ray spectra analyzed by Takei et al. (2009) suggested oxygen/neon-rich ejecta. If so, the WD mass is decreasing and, as a result, V2491 Cyg is not a candidate of Type Ia supernova progenitors.

3. MAGNETIC ACTIVITY (V2491 CYG)

V2491 Cyg shows a single secondary maximum in the optical and near IR light curves, which we cannot reproduce by our evolution model. Here we propose magnetic activities as a new energy source of the secondary maximum.

The prenova X-ray was detected in V2491 Cyg with *Swift* (Ibarra & Kuulkers 2008). Ibarra et al. (2008) suggested that the prenova X-ray spectra are more like those seen from magnetic rather than non-magnetic cataclysmic variables. Takei et al. (2009) reported the first detection of superhard X-rays (15–60 keV) with the *Suzaku* HXD at day 10, the spectrum of which has a power law distribution, suggesting a non-thermal origin, and unlikely to arise from thermal emission from internal shocks. This superhard component was not seen in their second *Suzaku* observation at day 30. These two observations point toward strong magnetic activities on the WD surface.

Therefore, our idea on the secondary maximum is based on additional energy release associated with rotating magnetic field. We assume that V2491 Cyg is a polar system with magnetic field as strong as $B_0 \sim 10^7$ G on the WD surface (e.g., Warner 1995). Before the nova outburst, the WD magnetic field rotates synchronously with the WD spin as well as the binary orbital motion. After the outburst, the nova envelope expands largely and rotates differentially due to local angular momentum conservation. Then, the magnetic field no more rotates synchronously with the WD spin because the magnetic tension is not strong enough to keep the whole envelope rotating with the WD spin. We expect that the differential rotation amplifies magnetic field which drives strong magnetic activities. As the nova outburst proceeds, the density of the WD envelope is gradually decreasing due mainly to wind mass loss and then the magnetic field eventually recovers synchronous rotation. The strong magnetic activities end at this stage, cor-

TABLE 1
EPOCH OF SECONDARY MAXIMUM IN OUR NOVA MODELS

object	max ^a (day)	P_{orb} (day)	M_2^b (M_{\odot})	a (R_{\odot})	M_{WD} (M_{\odot})	$\varepsilon_{\text{rot}} \approx \varepsilon_{\text{mag}}$ (day)
V2491 Cyg	15	0.0958	0.18	1.0	1.32	13
					1.3	15
					1.27	18
V1493 Aql	50	0.156	0.34	1.4	1.2	40
					1.15	49
					1.1	62
V2362 Cyg	250	0.207	0.48	1.6	0.75	200
					0.7	240
					0.65	330

^a epoch of secondary maximum ^b calculated from equation (5)

responding to the end of a secondary maximum. Since the additional energy source disappears, the light curve goes back to a “normal” one as shown in Figure 1.

To confirm this idea we estimate the total thermal energy of gas plus radiation ($\varepsilon_{\text{th}} = \varepsilon_{\text{th,gas}} + \varepsilon_{\text{th,rad}}$), rotational kinetic energy ε_{rot} , wind kinetic energy $\varepsilon_{\text{wind}}$, and magnetic energy ε_{mag} , which are calculated from

$$\varepsilon_{\text{th}} = \varepsilon_{\text{th,gas}} + \varepsilon_{\text{th,rad}} = \frac{3}{2} \frac{kT}{\mu m_H} \rho + aT^4, \quad (1)$$

$$\varepsilon_{\text{rot}} = \frac{1}{2} \rho (r \Omega_{\text{spin}})^2, \quad (2)$$

$$\varepsilon_{\text{wind}} = \frac{1}{2} \rho v_{\text{wind}}^2, \quad (3)$$

$$\varepsilon_{\text{mag}} = \frac{B_0^2}{8\pi} \left(\frac{r}{R_{\text{WD}}} \right)^{-4}. \quad (4)$$

The temperature T , density ρ , and wind velocity v_{wind} are taken from our wind solutions of the best-fit model of V2491 Cyg ($1.3 M_{\odot}$ WD). Here we assume the dipole magnetic field of $B_0 = 3 \times 10^7$ G at the WD surface (e.g., Warner 1995, for V1500 Cyg) and that the WD spin period is the same as the orbital period, $2\pi/\Omega_{\text{spin}} = P_{\text{spin}} = P_{\text{orb}}$. Figure 2 shows the energy densities for five sequential stages during the nova outburst. The first model (*thick solid*) has the largest photospheric radius and corresponds to a stage at/near the optical maximum. We see that at/near the optical maximum, $\varepsilon_{\text{mag}} \lesssim \varepsilon_{\text{rot}}$ at $r \gtrsim 2 \times 10^9$ cm. This indicates that the magnetic field is differentially rotating outside of $r \sim 2 \times 10^9$ cm. Then, the rotation energy density decreases with time and eventually ε_{mag} becomes comparable to ε_{rot} at the stage of the smallest photospheric radius. After that, the magnetic field probably gains synchronous rotation with the WD spin. We expect that the magnetic activities have a peak at $\varepsilon_{\text{mag}} \approx \varepsilon_{\text{rot}}$. This condition is satisfied at day 15 for our best-fit model, being very consistent with the time of the secondary maximum.

Next we estimate the epoch when the companion emerges from the nova envelope. If the mass of the donor star is estimated from Warner’s (1995) empirical formula, i.e.,

$$\frac{M_2}{M_{\odot}} \approx 0.065 \left(\frac{P_{\text{orb}}}{\text{hours}} \right)^{5/4}, \quad \text{for } 1.3 < \frac{P_{\text{orb}}}{\text{hours}} < 9 \quad (5)$$

we have $M_2 = 0.18 M_{\odot}$, which corresponds to the separation of $a = 1.0 R_{\odot}$, and the effective Roche lobe radius of the primary component (WD) of $R_1^* = 0.55 R_{\odot}$. When the photospheric radius of the nova envelope shrinks to near the orbit (the separation a), the condition of $\varepsilon_{\text{rot}} < \varepsilon_{\text{mag}}$ is satisfied as shown in Figure 2. This indicates that the epoch

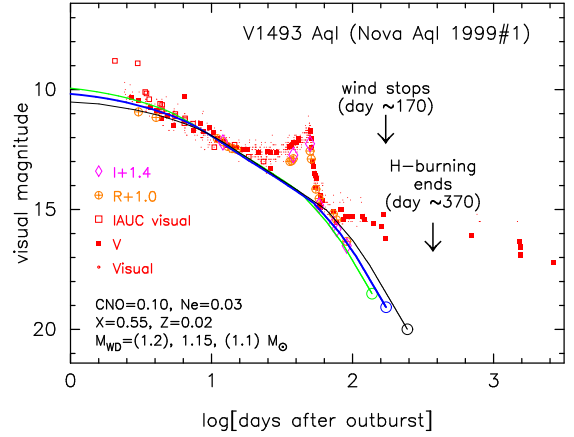


FIG. 3.— Same as Fig. 1, but for V1493 Aql (Nova Aql 1999 No.1). Our best-fit model is $M_{\text{WD}} = 1.15 M_{\odot}$ for the envelope chemical composition of $X = 0.55$, $Y = 0.30$, $X_{\text{CNO}} = 0.10$, $X_{\text{Ne}} = 0.03$, and $Z = 0.02$. Observational data are taken from AAVSO and VSOLJ. We further add the data of IAU Circ. 7223, 7225, 7228, 7232, 7258, 7273, 7313.

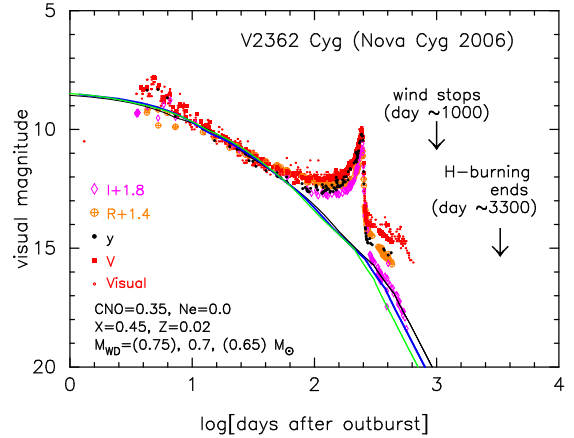


FIG. 4.— Same as Fig. 1, but for V2362 Cyg (Nova Cyg 2006). Our best-fit model is $M_{\text{WD}} = 0.7 M_{\odot}$ for the envelope chemical composition of $X = 0.45$, $Y = 0.18$, $X_{\text{CNO}} = 0.35$, and $Z = 0.02$. Observational data are taken from AAVSO and VSOLJ.

of the secondary maximum is shortly after the companion emerges from the nova envelope. We here implicitly assume that strong magnetic field connects the WD and the companion (like in polar systems). The mechanism of activity we suppose is magnetic reconnection. Strong magnetic reconnection occurs between the WD and the companion. When the WD photosphere is larger than the companion’s orbit, magnetic reconnection may occur deep inside the photosphere but the gas pressure (or gas thermal energy) at the reconnection region is much larger than the magnetic pressure (magnetic energy), so the gas is not easily accelerated by magnetic force. On the other hand, when the gas pressure becomes smaller than the magnetic pressure, i.e., when the photosphere shrinks to the orbit (see Fig.2), then the gas is easily accelerated by magnetic force and the envelope gas is massively ejected. Thus this process increases the mass-loss rate around/near the secondary maximum.

4. V1493 AQL AND V2362 CYG

V1493 Aql was discovered by Tago at mag 8.8 on July 13.558 UT. The nova was not detected on his films of July 5 and 9 (limiting mag 11 and 10.5, respectively). Therefore, we assume here that the outburst day is $t_{\text{OB}} = 2451372.0$ (July 12.5 UT). Figure 3 shows optical and near infrared light

curves of V1493 Aql. Our theoretical light curves of free-free emission reasonably fit with the observation until day ~ 100 except the secondary maximum. The best-fit model is the WD mass of $1.15 \pm 0.05 M_{\odot}$ for the chemical composition of $X = 0.55$, $Y = 0.30$, $X_{\text{CNO}} = 0.10$, $X_{\text{Ne}} = 0.03$, and $Z = 0.02$. The V and visual magnitudes deviate from our model light curve about 100 days after the outburst. This is due probably to the contribution of emission lines such as [O III] in the nebular phase. The orbital period of $P_{\text{orb}} = 0.156$ days was obtained by Dobrotka et al. (2006) from the modulations with a very small amplitude of 0.015 mag. The mass of the donor star is estimated to be $M_2 = 0.34 M_{\odot}$ from equation (5). The corresponding separation is $a = 1.4 R_{\odot}$ and the effective radius of the WD Roche lobe is $R_1^* = 0.68 R_{\odot}$. We have obtained the epoch of $\varepsilon_{\text{mag}} \approx \varepsilon_{\text{rot}}$ to be day 49 for our $1.15 M_{\odot}$ WD model as listed in Table 1. This timescale is consistent with the peak of the secondary maximum and also the emergence of the companion star from the WD envelope.

V2362 Cyg was discovered by Nishimura at mag 10.5 on 2006 April 2.807 UT. The nova was not detected on his films taken on March 28 (limiting mag 12) or on earlier patrol films back to 2001. Therefore, we assume here the outburst day of $t_{\text{OB}} = 2453827.0$ (April 1.5 UT). Optical and near infrared light curves are plotted in Figure 4. Our theoretical light curves of free-free emission again reasonably fit with the I observation until day ~ 500 except the secondary maximum. The best-fit model is the WD mass of $0.7 \pm 0.05 M_{\odot}$ for the chemical composition of $X = 0.45$, $Y = 0.18$, $X_{\text{CNO}} = 0.35$, and $Z = 0.02$ (see, e.g., Munari et al. 2008, for observed values). The R and y magnitudes slightly but the V and visual magnitudes largely deviate from our model light curve after the secondary maximum. The orbital period of $P_{\text{orb}} = 0.207$ days was obtained by Goranskij et al. (2008) from the modulations with an amplitude of 0.11 mag. If we take the donor mass of $M_2 = 0.48 M_{\odot}$ from equation (5), the separation is

$a = 1.6 R_{\odot}$, and the WD Roche lobe is $R_1^* = 0.66 R_{\odot}$. We have examined the epoch of $\varepsilon_{\text{mag}} \approx \varepsilon_{\text{rot}}$ to be day 240 for our model of $0.7 M_{\odot}$ WD as listed in Table 1. This timescale is again reasonably consistent with the peak of the secondary maximum and also the emergence of the companion star from the WD envelope.

5. CONCLUSIONS

We have estimated the WD mass of the classical novae V2491 Cyg by comparing our free-free light curves with the optical and near infrared observations as well as by comparing our blackbody X-ray light curves with the *Swift* XRT data. The best-fit model is the $1.3 \pm 0.02 M_{\odot}$ WD for the chemical composition of $X = 0.20$, $Y = 0.48$, $X_{\text{CNO}} = 0.20$, $X_{\text{Ne}} = 0.10$, and $Z = 0.02$. We strongly recommend composition analysis of the ejecta because the enrichment of WD matter provides information whether the WD mass increases or not. We have also estimated the WD mass of V1493 Aql and V2362 Cyg to be $M_{\text{WD}} = 1.15 \pm 0.05$ and $0.7 \pm 0.05 M_{\odot}$, respectively. For these three novae, the epoch of secondary maximum is consistently explained by our magnetic activity model if the magnetic activity reaches maximum at $\varepsilon_{\text{mag}} \approx \varepsilon_{\text{rot}}$ in the WD envelope. We strongly recommend search for magnetic activities for these three novae even in quiescence.

We thank D. Takei for providing us with their machine readable X-ray data of V2491 Cyg and also AAVSO and VSOLJ for the optical and near infrared data for V2491 Cyg, V1493 Aql, and V2362 Cyg. We are grateful to the anonymous referee for useful comments and to D. Takei, M. Tsujimoto, and S. Kitamoto for stimulating discussion on V2491 Cyg. This research has been supported in part by the Grant-in-Aid for Scientific Research (20540227) of the Japan Society for the Promotion of Science.

REFERENCES

- Baklanov, A., Pavlenko, E., & Berezina, E. 2008, *The Astronomer's Telegram*, 1514
- Bonifacio, P., Selvelli, P. L., & Caffau, E. 2000, *A&A*, 356, L53
- Dobrotka, A., Friedjung, M., Retter, A., Hric, L., & Novak, R. 2006, *A&A*, 448, 1107
- Goranskij, P. V., Metlova, V. N., & Burenkov, N. A. 2008, *The Astronomer's Telegram*, 928, 1
- Hachisu, I., & Kato, M. 2001a, *ApJ*, 553, L161
- Hachisu, I., & Kato, M. 2001b, *ApJ*, 558, 323
- Hachisu, I., & Kato, M. 2003b, *ApJ*, 590, 445
- Hachisu, I., & Kato, M. 2004, *ApJ*, 612, L57
- Hachisu, I., & Kato, M. 2006, *ApJS*, 167, 59
- Hachisu, I., & Kato, M. 2007, *ApJ*, 662, 552
- Hachisu, I., Kato, M., & Cassatella, A. 2008, *ApJ*, 687, 1236
- Hachisu, I., Kato, M., Kato, T., & Matsumoto, K. 2000, *ApJ*, 528, L97
- Hachisu, I., Kato, M., & Luna, G. J. M. 2007, *ApJ*, 659, L153
- Hachisu, I., Kato, M., & Nomoto, K. 1996, *ApJ*, 470, L97
- Hachisu, I., Kato, M., & Nomoto, K. 1999a, *ApJ*, 522, 487
- Hachisu, I., Kato, M., Nomoto, K., & Umeda, H. 1999b, *ApJ*, 519, 314
- Hachisu, I., Kato, M., & Schaefer, B. E. 2003, *ApJ*, 584, 1008
- Ibarra, A., & Kuulkers, E. 2008, *The Astronomer's Telegram*, 1473, 1
- Ibarra, A., et al. 2008, *The Astronomer's Telegram*, 1478, 1
- Iglesias, C. A., & Rogers, F. J. 1996, *ApJ*, 464, 943
- Kato, M. 1983, *PASJ*, 35, 507
- Kato, M. 1997, *ApJS*, 113, 121
- Kato, M. 1999, *PASJ*, 51, 525
- Kato, M., & Hachisu, I., 1994, *ApJ*, 437, 802
- Kato, M., & Hachisu, I., 2007, *ApJ*, 657, 1004
- Kimeswenger, S., Dalnadar, S., Knapp, A., Schafer, J., Unterguggenberger, S., & Weiss, S. 2008, *A&A*, 479, L51
- Munari, U., et al. 2008, *A&A*, in press (arXiv:0810.2387)
- Nakano, S., Beize, J., Jin, Z.-W., Gao, X., Yamaoka, H., Haseda, K., Guido, E., Sostero, G., Klingenberg, G., & Kadota, K. 2008, *IAU Circ.*, 8934, 1
- Nakano, S., Tago, A., & Nakamura, A. 1999, *IAU Circ.*, 7223, 1
- Page, K. L., et al. 2009, in preparation
- Payne-Gaposchkin, C. 1957, *The Galactic Novae* (Amsterdam: North-Holland)
- Takei, D., Tsujimoto, M., Kitamoto, S., Ness, J.-U., Drake, J. J., & Takahashi, H. 2009, in preparation
- Tomov, T., Mikolajewski, M., Brozek, T., Ragan, E., Swierczynski, E., Wychudzi, P., & Galan, C. 2008, *The Astronomer's Telegram*, 1485
- Venturini, C. C., Rudy, R. J., Lynch, D. K., Mazuk, S., & Puetter, R. C. 2004, *AJ*, 128, 405
- Warner, B. 1995, *Cataclysmic variable stars*, Cambridge, Cambridge University Press